

Investigation of ferromagnetic filled skutterudite compounds $\text{EuT}_4\text{Sb}_{12}$ (T = Fe, Ru, Os)

This article has been downloaded from IOPscience. Please scroll down to see the full text article.

2004 J. Phys.: Condens. Matter 16 5095

(<http://iopscience.iop.org/0953-8984/16/28/027>)

View [the table of contents for this issue](#), or go to the [journal homepage](#) for more

Download details:

IP Address: 129.252.86.83

The article was downloaded on 27/05/2010 at 16:01

Please note that [terms and conditions apply](#).

Investigation of ferromagnetic filled skutterudite compounds $\text{EuT}_4\text{Sb}_{12}$ ($\text{T} = \text{Fe}, \text{Ru}, \text{Os}$)

E D Bauer^{1,5}, A Ślebarski^{1,6}, N A Frederick¹, W M Yuhasz¹, M B Maple¹, D Cao^{2,5}, F Bridges², G Giester³ and P Rogl⁴

¹ Department of Physics and Institute for Pure and Applied Physical Sciences, University of California, San Diego, La Jolla, CA 92093, USA

² Department of Physics, University of California, Santa Cruz, Santa Cruz, CA 92064, USA

³ Institut für Mineralogie and Kristallographie, Universität Wien, Althanstrasse 14, A-1090 Wien, Austria

⁴ Institut für Physikalische Chemie, Universität Wien, Althanstrasse 14, A-1090 Wien, Austria

Received 19 February 2004

Published 2 July 2004

Online at stacks.iop.org/JPhysCM/16/5095

doi:10.1088/0953-8984/16/28/027

Abstract

The physical properties of single crystals of filled skutterudite compounds $\text{EuT}_4\text{Sb}_{12}$ ($\text{T} = \text{Fe}, \text{Ru}, \text{Os}$) have been investigated by means of x-ray diffraction, electrical resistivity, specific heat, magnetization, and x-ray absorption spectroscopy measurements. The Eu-based materials crystallize in the $\text{LaFe}_4\text{P}_{12}$ -type structure (space group $Im\bar{3}$). A small Eu deficiency is encountered for $\text{Eu}_{0.95}\text{Fe}_4\text{Sb}_{12}$, while the homologous compounds, $\text{Eu}_{1.0}\text{Ru}_4\text{Sb}_{12}$ and $\text{Eu}_{1.0}\text{Os}_4\text{Sb}_{12}$, reveal full occupancy of the Eu site. $\text{Eu}_{0.95}\text{Fe}_4\text{Sb}_{12}$ appears to exhibit either canted ferromagnetic or ferrimagnetic order at $T_C = 88$ K whereas $\text{EuRu}_4\text{Sb}_{12}$ and $\text{EuOs}_4\text{Sb}_{12}$ are ferromagnets with Curie temperatures of $T_C = 4$ and 9 K, respectively. X-ray absorption near edge spectroscopy measurements reveal a nearly divalent Eu electronic configuration for $\text{EuT}_4\text{Sb}_{12}$ ($\text{T} = \text{Fe}, \text{Ru}, \text{Os}$) with no significant change with T atom or temperature.

1. Introduction

The filled skutterudites RT_4X_{12} ($\text{R} = \text{alkaline earth, rare earth, or actinide}$; $\text{T} = \text{Fe, Ru, or Os}$; $\text{X} = \text{P, As, or Sb}$) have received a large amount of attention in recent years due to the variety of strongly correlated electron ground states these materials display and also because of their possible use in thermoelectric applications [1, 2]. A host of phenomena are observed in these compounds such as superconductivity, magnetism, heavy fermion, intermediate valence, non-Fermi liquid, and small band gap semiconducting behaviour [3]. The filled skutterudite compounds crystallize in the BCC $\text{LaFe}_4\text{P}_{12}$ -type structure [4, 5] which is derived from the

⁵ Present address: Los Alamos National Laboratory, Los Alamos, NM 87545, USA.

⁶ On leave from: Institute of Physics, University of Silesia, 40-007 Katowice, Poland.

CoAs₃ structure by filling the available voids with the R atoms in the unit cell. The R atoms are situated in an oversized atomic cage formed by the T₄X₁₂ units. The wide range of hybridization between the R ions and the TX₃ polyanions leads to the large variety of thermodynamic and transport behaviours. These materials can be synthesized by conventional means with rare earth elements R = La–Eu, Yb; the skutterudites with R = Y, Gd, and Tb are formed only under large pressures up to 50 kbar [6, 7]. The absence of the compounds with heavier rare earths (with the exception of Yb) is due presumably to the inadequate bonding of the heavier (smaller) R³⁺ ions to the neighbouring ions in the somewhat rigid cages in the TX₃ structure. However, both Eu and Yb are close to a valence instability and often form compounds which exhibit intermediate valence characteristics [8]. Therefore, the filled skutterudite structure is stabilized with these two rare earth elements having either a divalent configuration (which is larger in size than the trivalent configuration) or a mixture of divalent and trivalent states.

The ferromagnetic filled skutterudite EuFe₄Sb₁₂ has unusual magnetic properties, characterized by a low saturation moment and a large Curie temperature, compared to other magnetically ordered skutterudites. Magnetic measurements on polycrystalline samples of EuFe₄Sb₁₂ by Danebrock *et al* [9] yielded a surprisingly low value of the saturation moment of $\mu_{\text{sat}} = 4.9 \mu_{\text{B}}/\text{Eu}$ (5 K), compared with the expected value for Eu²⁺ (identical to that of Gd³⁺, $J = S = 7/2$) of $M = gJ = 7.0 \mu_{\text{B}}$. In addition, after subtracting the magnetic susceptibility of CaFe₄Sb₁₂ to account for the (Fe₄Sb₁₂) polyanion contribution ($\mu_{\text{eff}}^{\text{poly}} = 2.6 \mu_{\text{B}}$), an effective moment of $\mu_{\text{eff}}^{\text{Eu}} = 6.8 \mu_{\text{B}}/\text{Eu}$ was obtained which is also lower than expected for Eu²⁺ ($\mu_{\text{eff}}^{\text{Eu}^{2+}} = 7.94 \mu_{\text{B}}$). Further investigations on polycrystalline samples of EuFe₄Sb₁₂ [10] revealed a partial occupancy of 83% of the Eu sites for this material. Magnetic susceptibility measurements revealed an effective moment $\mu_{\text{eff}} = 7.28 \mu_{\text{B}}/\text{fu}$ consistent with either the reduced Eu²⁺ occupancy or a Eu valence of $\nu \sim 2.15$ at full Eu site occupancy. On the basis of the reduced saturation moment $\mu_{\text{sat}} = 3.55 \mu_{\text{B}}/\text{Eu}$ (2 K), the authors suggested either canted ferromagnetic or ferrimagnetic order below $T_{\text{C}} = 84$ K for EuFe₄Sb₁₂ [10]. From magnetization and specific heat measurements on polycrystalline samples, EuRu₄Sb₁₂ was found to order ferromagnetically at $T_{\text{C}} = 3.3$ K with a saturation moment $\mu_{\text{sat}} = 6.2 \mu_{\text{B}}/\text{Eu}$ (2.1 K) and an effective moment of $\mu_{\text{eff}}^{\text{Eu}} = 7.2 \mu_{\text{B}}/\text{Eu}$ [11]. The saturation moment and reduced entropy ($\sim 15 \text{ J mol}^{-1} \text{ K}^{-2}$ just above the ferromagnetic transition) are consistent with a mixed valence state of Eu with $\nu \sim 2.1$.

Some of these apparent discrepancies may arise from inhomogeneities in the polycrystalline samples. We have therefore carried out an investigation of single-crystal specimens of EuT₄Sb₁₂ (T = Fe, Ru, Os) filled skutterudite compounds. Our results indicate EuFe₄Sb₁₂ and EuRu₄Sb₁₂ order magnetically at 89 and 4 K, respectively, and their physical properties are generally consistent with those of the polycrystalline samples previously reported [9–11]. The physical properties of EuOs₄Sb₁₂ have been investigated for the first time; our measurements show that this compound also exhibits ferromagnetic order with a Curie temperature $T_{\text{C}} = 9$ K.

2. Experimental details

Single crystals of the EuT₄Sb₁₂ compounds were prepared by a metal flux growth method with Sb flux. High purity starting materials (Eu: Ames Lab, 4N; T: Colonial Metals, 3N; Sb: Alfa Aesar, 6N) were placed in the ratio Eu:T:Sb = 1:4:20 in evacuated carbon coated quartz tubes, heated to 950 °C for 24 h, and then cooled slowly ($\sim 3 \text{ }^\circ\text{C h}^{-1}$) to 650 °C; this was followed by a quench ($\sim 200 \text{ }^\circ\text{C h}^{-1}$) to room temperature. The specimens were removed from the excess antimony flux by etching in aqua regia (3:1 = HCl:HNO₃). The crystals were usually cubic or rectangular in shape and ranged from 0.1 to 5 mm in the largest dimension.

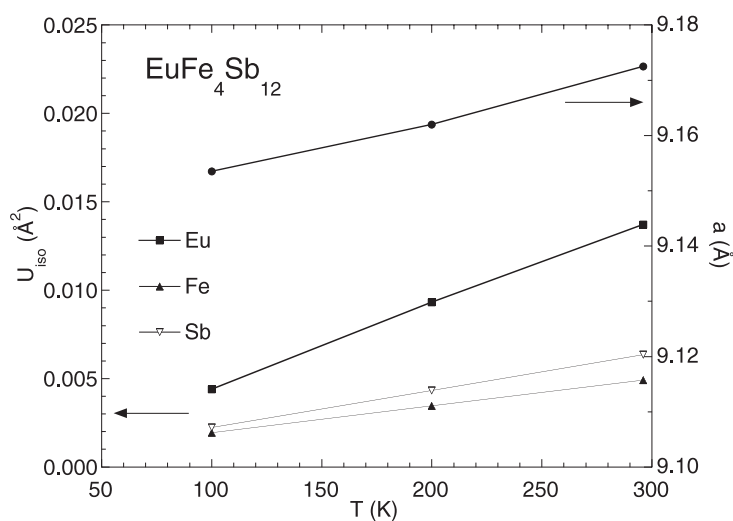


Figure 1. The lattice parameter a (right axis) and isotropic thermal displacement factors U_{iso} (left axis) of Eu, Fe, and Sb versus temperature T of $\text{Eu}_{0.95}\text{Fe}_4\text{Sb}_{12}$.

Single-crystal x-ray intensity data were collected with a minimum redundancy level of better than 10 on a four-circle Nonius Kappa diffractometer equipped with a CCD area detector employing graphite monochromated Mo $K\alpha$ radiation ($\lambda = 0.71073 \text{ \AA}$). A continuous stream of nitrogen gas at a preset temperature enclosing the crystal, mounted with Apiezon 4 grease on a glass rod, was used for temperature dependent measurements down to 100 K. The absorption correction was taken from the program SORTAV [12] and the structures were refined with the aid of the SHELXS-97 program [13].

Magnetization measurements were performed in a Quantum Design MPMS magnetometer from 1.8 to 300 K in magnetic fields up to 5.5 T on a collection of single crystals. The electrical resistivity was measured in a commercial Quantum Design PPMS cryostat from 1.8 to 300 K using a standard four-wire technique with excitation currents from 1 to 10 mA. Specific heat measurements were made in a He^3 calorimeter using a standard heat-pulse technique on pressed pellets of powdered single crystals.

X-ray absorption near edge spectroscopy (XANES) experiments were carried out on beam line 4-3 at Stanford Synchrotron Radiation Laboratory (SSRL) using silicon (220) monochromator crystals. Eu L_{III} transmission data were taken as a function of temperature with EuF_2 , EuF_3 , and Eu_2O_3 as valence reference compounds. A 400-mesh sieve was used after the single-crystal samples were ground to obtain a very fine powder which was then brushed onto Scotch tape. One double layer of each sample (sample thickness is ~ 0.2 absorption lengths for Eu) was used when collecting XANES data. A pre-edge background (contribution from other edges) was subtracted for all the XANES data using standard procedures [14, 15]. The step height of the main absorption edge was normalized to 1 for each of the samples and references.

3. Results

3.1. Single-crystal structural refinements

Structural refinements on single crystals of $\text{EuT}_4\text{Sb}_{12}$ have been performed and the results are listed in table 1. The cubic lattice parameters and thermal displacement parameters (U_{iso}) as a function of temperature of $\text{Eu}_{0.95}\text{Fe}_4\text{Sb}_{12}$ are shown in figure 1 and display a monotonic,

Table 1. Single-crystal structural data for EuT₄Sb₁₂ (T = Fe, Ru, Os) compounds; LaFe₄P₁₂ type; space group $Im\bar{3}$ (No 204); range of scattering angle $2 < 2\theta < 80$.

Parameter	Compound				
	EuFe ₄ Sb ₁₂	EuRu ₄ Sb ₁₂	EuOs ₄ Sb ₁₂	EuFe ₄ Sb ₁₂	EuOs ₄ Sb ₁₂
<i>T</i> (K)	296	200	100	296	296
Lattice parameter, <i>a</i> (Å)	9.1725(2)	9.1620(2)	9.1535(2)	9.2877(2)	9.3255(2)
Density, ρ (g cm ⁻³)	7.903	7.930	7.952	8.362	9.721
Reflections measured	426	430	433	447	443
Number of variables	12	12	12	11	11
$R_{F^2} = \sum F_o^2 - F_c^2 / \sum F_o^2$	0.0225	0.0198	0.0196	0.0184	0.0212
GOF χ^2	1.274	1.246	1.226	1.203	1.209
Atom parameters					
Eu in site 2a (0, 0, 0);					
Occupancy	0.957(4)	0.959(4)	0.949(4)	1.00(1)	1.00(1)
Isotropic thermal parameter, U_{iso} (Å ²)	0.0136(2)	0.0095(2)	0.0043(2)	0.0157(1)	0.0179(2)
T in site 8c (1/4, 1/4, 1/4);					
Occupancy	1.0(1)	1.0(1)	1.0(1)	1.0(1)	1.0(1)
U_{iso} (Å ²)	0.0049(2)	0.0034(1)	0.0019(1)	0.0042(1)	0.0033(1)
Sb in site 24g (0, <i>y</i> , <i>z</i>); <i>y</i> :					
	0.160 19(2)	0.160 14(2)	0.160 10(2)	0.158 07(2)	0.156 25(2)
<i>z</i> :	0.337 59(2)	0.337 63(2)	0.337 68(2)	0.342 73(2)	0.341 13(3)
Occupancy	1.0(1)	1.0(1)	1.0(1)	1.0(1)	1.0(1)
U_{11} (Å ²)	0.0049(1)	0.0033(1)	0.0017(1)	0.0043(1)	0.0034(1)
U_{22} (Å ²)	0.0065(1)	0.0043(1)	0.0022(1)	0.0062(1)	0.0052(1)
U_{33} (Å ²)	0.0076(1)	0.0052(1)	0.0028(1)	0.0068(1)	0.0064(1)
Interatomic distances (Å) (uncertainties generally <0.0001 Å)					
Eu–12Sb	3.4274	3.4237	3.4207	3.5054	3.4990
T–6Sb	2.5656	2.5630	2.5609	2.6195	2.6310
Sb–1Eu	3.4274	3.4237	3.4207	3.5054	3.4990
Sb–2T	2.5656	2.5630	2.5609	2.6195	2.6310
Sb–1Sb	2.9386	2.9345	2.9309	2.9214	2.9142
Sb–1Sb	2.9794	2.9753	2.9716	2.9362	2.9630

practically linear T -dependence in the measured temperature interval from 100 to 296 K. At all temperatures, the values U_{iso} for Eu are significantly larger than those found for the Fe₄Sb₁₂ framework atoms. Large thermal displacement parameters have been observed in the filled skutterudites [4, 16]; the ‘rattling’ of these R atoms is believed to scatter phonons effectively, leading to a reduction of the lattice thermal conductivity and, hence, enhanced thermoelectric properties. It is interesting to note that the light Fe atoms, caged in the heavy octahedral Sb units, show smaller thermal displacement parameters than their cage units. This is in agreement with a strong Fe–Sb bond as seen from the bond length of Fe–Sb, which is shorter by about 10% with respect to the Sb–Sb bonds. Considering the crystal as a simple Debye solid with a ‘rattling’ Eu atom in site 2a as a single-harmonic Einstein oscillator, in which

$$U_{iso} = \frac{h^2}{8\pi^2 m k_B \theta_E} \coth\left(\frac{\theta_E}{2T}\right), \quad (1)$$

where the reduced mass m is assumed to be the atomic mass of Eu (rigid cage approximation), k_B is the Boltzmann constant, and θ_E is the Einstein temperature, we extract from the linear

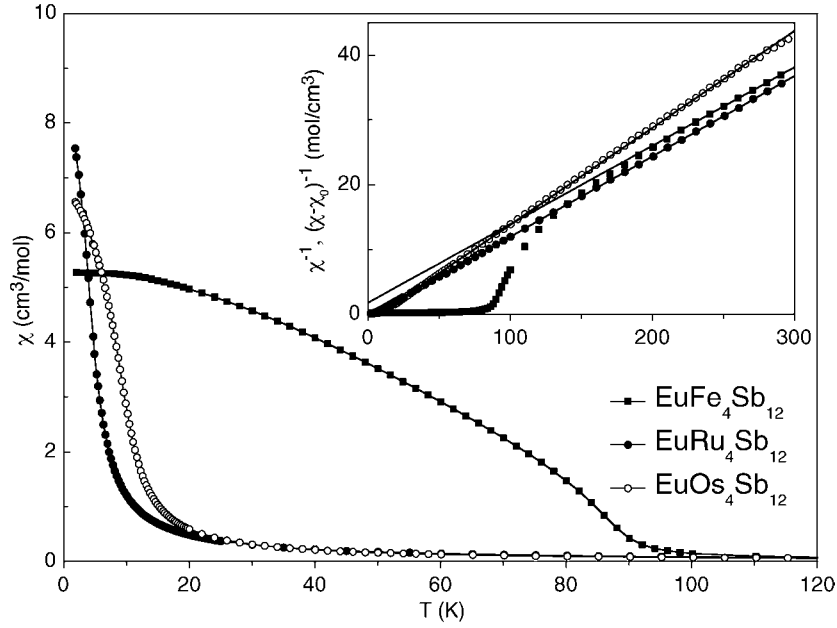


Figure 2. Magnetic susceptibility $\chi \equiv M/H$ versus temperature T in a magnetic field of $H = 0.5$ T for the $\text{EuT}_4\text{Sb}_{12}$ ($T = \text{Fe, Ru, Os}$) compounds. Inset: inverse magnetic susceptibility χ^{-1} ($(\chi - \chi_0)^{-1}$ for $\text{Eu}_{0.95}\text{Fe}_4\text{Sb}_{12}$) versus T . The lines are fits of a Curie–Weiss law to the data.

slope $\Delta U_{\text{iso}}/\Delta T$ in figure 1 the force constant $K = 4\pi^2 m v_{\text{Eu}}^2 = 29\,084 \text{ g s}^{-2}$, the frequency of vibration $\nu_{\text{Eu}} = 1.71 \times 10^{12} \text{ s}^{-1}$, and, hence, an Einstein temperature $\theta_{\text{E}} = 82$ K. Comparable Einstein temperatures of $\theta_{\text{E}} = 78$ and 74 K for $\text{EuRu}_4\text{Sb}_{12}$ and $\text{EuOs}_4\text{Sb}_{12}$, respectively, are found using equation (1) and the values of the room temperature U_{iso} data are listed in table 1. These Einstein temperatures for the Eu-based filled skutterudites are in excellent agreement with those obtained from recent x-ray absorption fine structure measurements [17]. Low frequency rattling modes of comparable magnitude have been observed in other filled skutterudites such as $\text{La}_{0.75}\text{Fe}_3\text{CoSb}_{12}$ and $\text{YbFe}_4\text{Sb}_{12}$ [16].

3.2. Magnetic measurements

The magnetic susceptibility $\chi \equiv M/H$ of each of the filled skutterudite compounds $\text{EuT}_4\text{Sb}_{12}$ ($T = \text{Fe, Ru, Os}$) in a magnetic field $H = 0.5$ T as a function of temperature is shown in figure 2. All three compounds exhibit a large increase in $\chi(T)$ below 100 K indicating ferromagnetism. The inverse magnetic susceptibility χ^{-1} is linear in temperature above 200 K for $\text{Eu}_{0.95}\text{Fe}_4\text{Sb}_{12}$ and over an extended temperature range of 20–300 K for $\text{EuRu}_4\text{Sb}_{12}$ and $\text{EuOs}_4\text{Sb}_{12}$. Least-squares fits to the data of a Curie–Weiss law

$$\chi(T) = \frac{C}{T - \theta_{\text{CW}}}, \quad (2)$$

with $C = N_A \mu_{\text{eff}}^2 / 3k_{\text{B}}$, where N_A is Avogadro's number and μ_{eff} is the effective moment, yield $\mu_{\text{eff}} = (8.4, 8.0, 7.3) \mu_{\text{B}}$ and $\theta_{\text{CW}} = (-18, 3, 8)$ K for $\text{EuT}_4\text{Sb}_{12}$ ($T = \text{Fe, Ru, Os}$), respectively. (An empirical modified Curie–Weiss law, i.e., $\chi(T) = \chi_0 + C/(T - \theta_{\text{CW}})$, was used to account for the strong ferromagnetic correlations in $\text{Eu}_{0.95}\text{Fe}_4\text{Sb}_{12}$.) These effective

Table 2. Physical properties of $\text{EuT}_4\text{Sb}_{12}$ ($T = \text{Fe, Ru, Os}$) compounds. T_C —Curie temperature; μ_{eff} —effective moment; θ_{CW} —Curie–Weiss temperature; μ_{sat} —saturation moment at $T = 1.8$ K; γ —electronic specific heat coefficient; θ_D —Debye temperature; θ_E —Einstein temperature. The values of the effective moment $\mu_{\text{eff}}^{\text{Eu}}$ and Curie–Weiss temperature θ_{CW} were obtained from fits of the high temperature magnetic susceptibility to equation (2) (or equation (3) for $\text{Eu}_{0.95}\text{Fe}_4\text{Sb}_{12}$). The electronic specific heat coefficient γ and Debye temperature θ_D were determined from fits to the low temperature specific heat. The Einstein temperature θ_E was calculated from equation (1) using the values of the thermal displacement parameters listed in table 1 at $T = 296$ K.

Compound	$\mu_{\text{eff}}^{\text{Eu}}$ ($\mu_B/\text{Eu atom}$)	θ_{CW} (K)	T_C (K)	μ_{sat} ($\mu_B/\text{Eu atom}$)	γ ($\text{mJ mol}^{-1} \text{K}^{-2}$)	θ_D (K)	θ_E (K)
$\text{Eu}_{0.95}\text{Fe}_4\text{Sb}_{12}$	7.7	−18	87	5.1	85 (~ 100) ^a	348 ^a	84
$\text{EuRu}_4\text{Sb}_{12}$	8.0	3	4	7.3	73	262	78
$\text{EuOs}_4\text{Sb}_{12}$	7.3	8	9	6.0	135	304	74

^a From [10].

moments are reasonably close to the expected value for divalent Eu^{2+} of $\mu_{\text{eff}}^{\text{Eu}^{2+}} = 7.94 \mu_B$. For $\text{Eu}_{0.95}\text{Fe}_4\text{Sb}_{12}$, however, it is expected that the measured μ_{eff} consists of a contribution from the magnetic ($\text{Fe}_4\text{Sb}_{12}$) polyanions. Assuming that the contributions to the magnetic susceptibility of the Eu ions and the ($\text{Fe}_4\text{Sb}_{12}$) polyanions are additive and have the same T -dependence, the magnetic moment of $\text{Eu}_{0.95}\text{Fe}_4\text{Sb}_{12}$ is given by

$$\mu_{\text{eff}}^{\text{meas}} = \sqrt{0.95(\mu_{\text{eff}}^{\text{Eu}})^2 + (\mu_{\text{eff}}^{\text{poly}})^2}. \quad (3)$$

The effective moment of the magnetic polyanions was represented by that of $\text{SrFe}_4\text{Sb}_{12}$, due to the similarities between $\text{SrFe}_4\text{Sb}_{12}$ and $\text{Eu}_{0.95}\text{Fe}_4\text{Sb}_{12}$: in both compounds, the filling atom is divalent (see [9] and section 3.5, respectively), and the Curie–Weiss temperatures are nearly identical (−17 and −18 K, respectively). This effective moment, $\mu_{\text{eff}}^{\text{poly}} = 3.8 \mu_B$ [9], was substituted in equation (3) and resulted in a value of the measured effective moment of $\mu_{\text{eff}}^{\text{Eu}} = 7.7 \mu_B$, a value closer to that expected for Eu^{2+} ($\mu_{\text{eff}}^{\text{Eu}^{2+}} = 7.94 \mu_B$). Both $\text{EuRu}_4\text{Sb}_{12}$ and $\text{EuOs}_4\text{Sb}_{12}$ exhibit typical ferromagnetic behaviour in which the effective moment is also close to that expected for Eu^{2+} and the Curie–Weiss temperature is comparable to the Curie temperature. The magnetic ordering temperatures of $T_C = 87, 4,$ and 9 K, for $\text{EuT}_4\text{Sb}_{12}$ ($T = \text{Fe, Ru, Os}$), respectively, determined from the peak in $d\chi/dT$ (not shown) are consistent with specific heat and electrical resistivity measurements discussed below (results listed in table 2).

The isothermal magnetization M versus H is shown for $\text{EuT}_4\text{Sb}_{12}$ ($T = \text{Fe, Ru, Os}$) in figures 3(a)–(c), respectively. By extrapolating the high field slope of the magnetization curves at 1.8 K (5 K for $\text{Eu}_{0.95}\text{Fe}_4\text{Sb}_{12}$), the saturation moment μ_{sat} was determined as ($5.1 (=4.8/0.95), 7.3, 6.0$) $\mu_B/\text{Eu atom}$ for the $\text{EuT}_4\text{Sb}_{12}$ ($T = \text{Fe, Ru, Os}$) compounds, respectively. The reduced saturation moment and the s-shaped curvature of $\chi^{-1}(T)$, consistent with previous measurements [9, 10], suggest ferrimagnetic ordering of the Eu and Fe moments in $\text{Eu}_{0.95}\text{Fe}_4\text{Sb}_{12}$, although a canted ferromagnetic alignment of the Eu moments cannot be ruled out.

3.3. Specific heat

The electrical and magnetic contributions to the specific heat for $\text{EuRu}_4\text{Sb}_{12}$ and $\text{EuOs}_4\text{Sb}_{12}$, ΔC versus T , determined by subtracting the lattice specific heat of $\text{LaRu}_4\text{Sb}_{12}$ ($\Theta_D = 262$ K) [18] and $\text{LaOs}_4\text{Sb}_{12}$ ($\Theta_D = 304$ K) [3], respectively, are shown in figure 4. The ferromagnetic transitions are clearly visible as peaks at ~ 3 and 8 K for $\text{EuRu}_4\text{Sb}_{12}$ and $\text{EuOs}_4\text{Sb}_{12}$, respectively, and the Curie temperatures, determined from the mid-point of

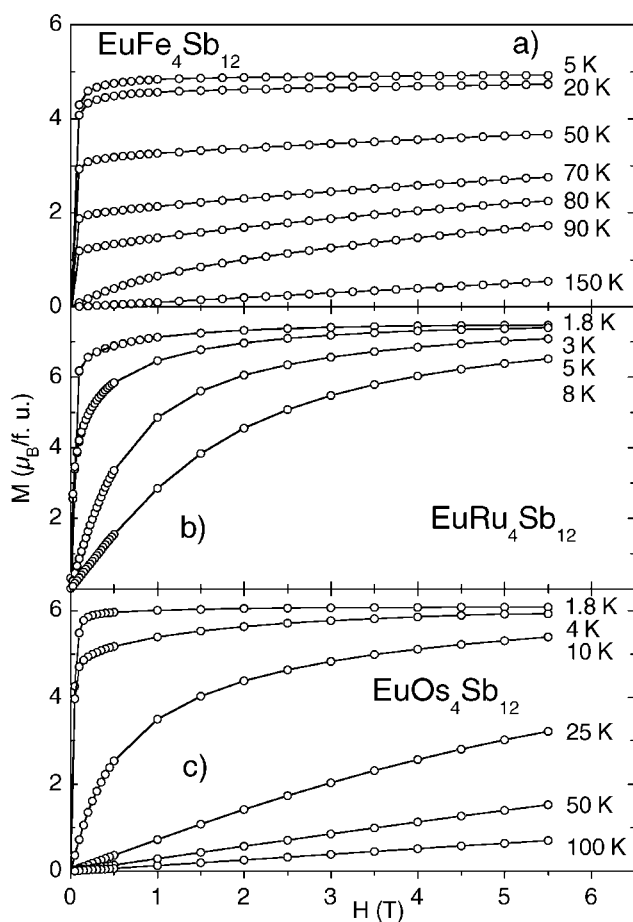


Figure 3. Isothermal magnetization M versus H for $\text{EuT}_4\text{Sb}_{12}$ ($T = \text{Fe, Ru, Os}$), shown in panels (a)–(c), respectively.

the jump in $\Delta C(T)$, are $T_C = 3.6$ and 8.5 K, respectively. Displayed in the inset to figure 4 is a plot of the specific heat C versus T associated with the magnetic transition of $\text{EuFe}_4\text{Sb}_{12}$. This transition temperature, taken to be the mid-point of the region with nearly zero slope, was determined as $T_C = 88$ K. Estimates of the electronic specific heat coefficient γ of $\text{EuRu}_4\text{Sb}_{12}$ and $\text{EuOs}_4\text{Sb}_{12}$ were obtained from plots of $\Delta C/T$ versus T^2 . A linear fit to the $\Delta C/T$ data above the ferromagnetic transition $8.5 \text{ K} \leq T \leq 12 \text{ K}$ ($12 \text{ K} \leq T \leq 14 \text{ K}$) yielded $73 \text{ mJ mol}^{-1} \text{ K}^{-2}$ ($135 \text{ mJ mol}^{-1} \text{ K}^{-2}$) for $\text{EuRu}_4\text{Sb}_{12}$ ($\text{EuOs}_4\text{Sb}_{12}$) once the electronic contribution of the La-based skutterudite was subtracted (results listed in table 2). An extrapolation of C/T to $T = 0 \text{ K}$ of $\text{Eu}_{0.95}\text{Fe}_4\text{Sb}_{12}$ yielded $\gamma \sim 85 \text{ mJ mol}^{-1} \text{ K}^{-2}$. These values of γ should be considered as an upper limit given the limited fit range and the use of a high temperature extrapolation and are probably more similar to those of $\text{LaRu}_4\text{Sb}_{12}$ and $\text{LaOs}_4\text{Sb}_{12}$ [3, 18]. It is interesting to note that the γ value of $\text{LaFe}_4\text{Sb}_{12}$ ($\gamma \sim 185 \text{ mJ mol}^{-1} \text{ K}^{-2}$ [10] and this work) is larger than those for the homologous $\text{LaRu}_4\text{Sb}_{12}$ and $\text{LaOs}_4\text{Sb}_{12}$ compounds that have $\gamma = 39$, and $36 \text{ mJ mol}^{-1} \text{ K}^{-2}$, respectively [3, 18]. Large values of the Sommerfeld coefficient $\gamma \sim 100 \text{ mJ mol}^{-1} \text{ K}^{-2}$ are also observed in the Fe-containing skutterudites $\text{NaFe}_4\text{Sb}_{12}$ and $\text{BaFe}_4\text{Sb}_{12}$, raising the

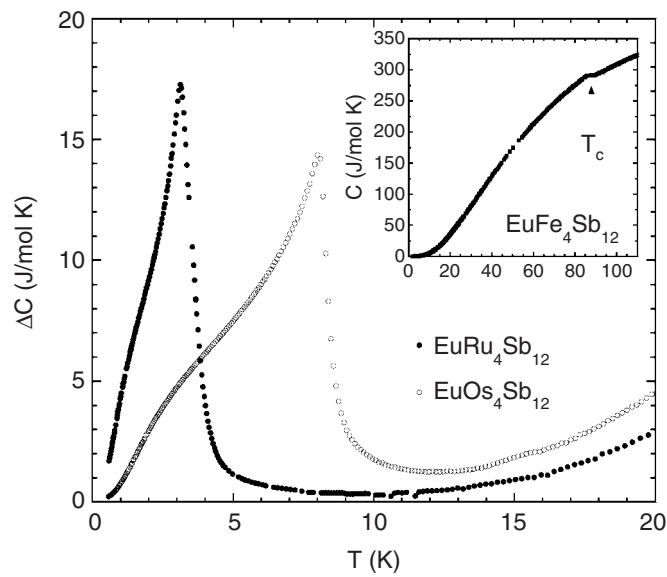


Figure 4. Magnetic specific heat ΔC versus temperature T for $\text{EuT}_4\text{Sb}_{12}$ ($T = \text{Ru, Os}$). Inset: the specific heat $C(T)$ of $\text{Eu}_{0.95}\text{Fe}_4\text{Sb}_{12}$.

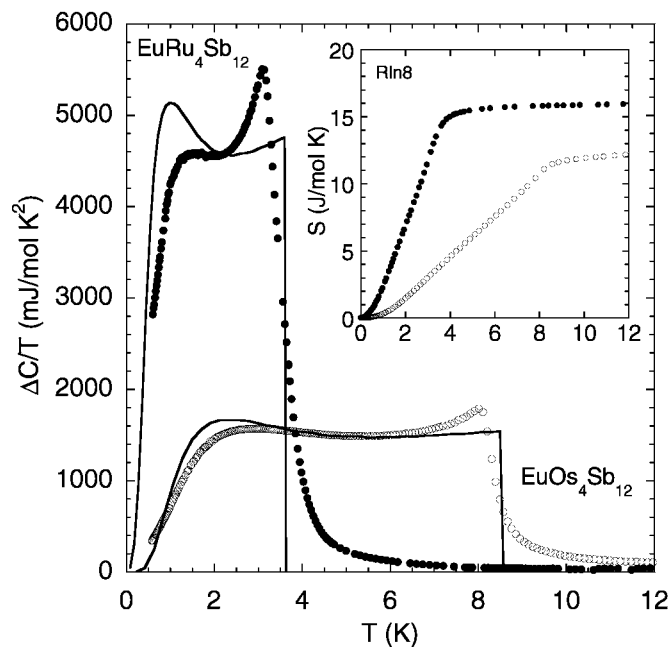


Figure 5. Magnetic specific heat divided by temperature $\Delta C/T$ versus T for $\text{EuRu}_4\text{Sb}_{12}$ (solid circles) and $\text{EuOs}_4\text{Sb}_{12}$ (open circles). The solid curves are MFT calculations discussed in section 3.3. Inset: magnetic entropy S versus T for $\text{EuRu}_4\text{Sb}_{12}$ (solid circles) and $\text{EuOs}_4\text{Sb}_{12}$ (open circles).

possibility of significant hybridization of the Fe d states with the conduction electrons [19]. As displayed in the inset of figure 5, the entropy $S = \int (\Delta C/T) dT$ (extrapolating a power

law T -dependence of $\Delta C/T$ below 0.6 K) attains a value $S \sim 16 \text{ J mol}^{-1} \text{ K}^{-1}$ for $\text{EuRu}_4\text{Sb}_{12}$ and $S \sim 12 \text{ J mol}^{-1} \text{ K}^{-1}$ for $\text{EuOs}_4\text{Sb}_{12}$ above the ferromagnetic transition. These values are lower than expected for Eu^{2+} ($S = R \ln(2J + 1) = 17.3 \text{ J mol}^{-1} \text{ K}^{-1}$) and may be reconciled by subtle differences in the phonon structure of the isomorphous La compounds, intermediate valence effects, and/or the presence of free Sb, judged to be less than 5% from x-ray powder diffraction analysis. On the other hand, the entropy of $\text{Eu}_{0.95}\text{Fe}_4\text{Sb}_{12}$ below 90 K, upon subtracting the specific heat of $\text{La}_{0.83}\text{Fe}_4\text{Sb}_{12}$ [10], is $S \sim 27 \text{ J mol}^{-1} \text{ K}^{-1}$, a larger value than expected for Eu^{2+} , although consistent with previous results [10].

Figure 5 shows $\Delta C/T$ versus T for $\text{EuRu}_4\text{Sb}_{12}$ and $\text{EuOs}_4\text{Sb}_{12}$, which both display a broad maximum below T_C ($T_{\text{max}} \approx 1.5$ and 2.9 K , respectively). The shapes of these maxima are similar to those of Schottky anomalies which often result from the splitting of the degenerate energy levels of rare earth ions in the crystalline electric field (CEF). However, the electronic configuration of Eu^{2+} with $J = S = 7/2$ and $L = 0$ should preclude CEF anomalies in this temperature range. Broad maxima are expected from mean field theory (MFT) within the ferromagnetic state when $S \geq 3$ [20]. Using MFT to solve for $C(T)$ when $S = 7/2$ gives rise to a peak in C/T at $T_{\text{max}} = 0.9 \text{ K}$ for $T_C = 3.6 \text{ K}$ and at $T_{\text{max}} = 2.3 \text{ K}$ for $T_C = 8.5 \text{ K}$, and reproduces the general features of the data, as shown in figure 5. A scaling factor of 0.85 (0.65) has been applied to the MFT result for $\text{EuRu}_4\text{Sb}_{12}$ ($\text{EuOs}_4\text{Sb}_{12}$) which is consistent with the reduced entropy and may be justified for the reasons mentioned above. The discrepancies between the positions of the peaks, the heights of the ferromagnetic transitions (which should be $20.1 \text{ J mol}^{-1} \text{ K}^{-1}$, regardless of T_C), as well as the total entropy (which should be equal to $R \ln 8 = 17.3 \text{ J mol}^{-1} \text{ K}^{-1}$ at T_C) could also be described by quantum fluctuations due to the transverse degrees of freedom in a Heisenberg ferromagnet [21]. Furthermore, quantitative agreement is not expected at low temperatures in the ferromagnetic state due to the presence of spin waves, which are not accounted for by MFT.

3.4. Electrical resistivity

The electrical resistivity, normalized to the room temperature value, $\rho/\rho(300 \text{ K})$ versus T for the $\text{EuT}_4\text{Sb}_{12}$ compounds is displayed in figure 6. The absolute magnitude of the resistivity could not be determined accurately due to the irregular shapes of the crystals. The $\text{EuT}_4\text{Sb}_{12}$ materials exhibit metallic behaviour and a kink in the $\rho(T)$ curves is observed at the Curie temperature. The mid-point of the increase in $d\rho/dT$ corresponds well to the Curie temperature, and values of $T_C = (89, 3, 7) \text{ K}$ were determined for $\text{EuT}_4\text{Sb}_{12}$ ($T = \text{Fe, Ru, Os}$), respectively, similar to the values obtained from other measurements discussed above. The resistivity of $\text{Eu}_{0.95}\text{Fe}_4\text{Sb}_{12}$ at low temperatures below T_C is consistent with the T^2 behaviour expected for electron-magnon scattering in the magnetic state.

3.5. X-ray absorption measurements

Figure 7 shows the Eu L_{III} edge absorption $\mu(E)$ data (panel (a)) as well as $d\mu/dE$ (panel (b)) for the three $\text{EuT}_4\text{Sb}_{12}$ ($T = \text{Fe, Ru, Os}$) samples and three other reference materials (EuF_2 , EuF_3 and Eu_2O_3). The shapes and the edge positions of the Eu L_{III} edge for the three filled skutterudites are very similar (figures 7(a), (b)), which indicates that the electronic environments of Eu in these three samples are nearly identical. The positions of the Eu edges for $\text{EuT}_4\text{Sb}_{12}$ ($T = \text{Fe, Ru, Os}$) are very close to that of EuF_2 (Eu^{2+}) and are about 10 eV below those for EuF_3 and Eu_2O_3 (Eu^{3+}), indicating that the Eu valence in the three skutterudites is predominantly $2+$. The amplitude of the second peak at 6983 eV increases slightly for $\text{EuT}_4\text{Sb}_{12}$ ($T = \text{Fe, Ru, Os}$), suggesting a small increase in the fraction of Eu^{3+} as the transition metal progresses from Fe to Ru to Os.

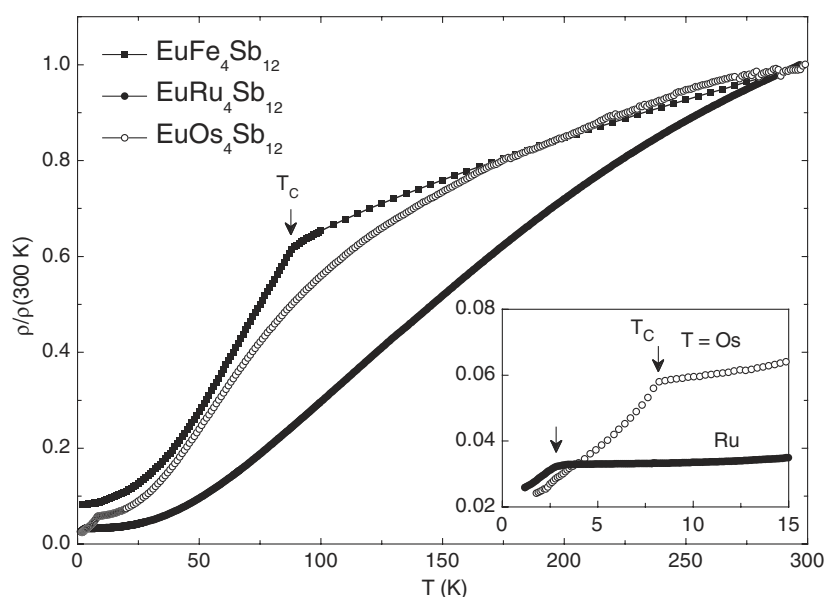


Figure 6. Normalized electrical resistivity $\rho/\rho(300\text{ K})$ versus temperature T for $\text{EuT}_4\text{Sb}_{12}$ ($T = \text{Fe, Ru, Os}$). Inset: the normalized electrical resistivity at low temperatures showing the ferromagnetic transitions of $\text{EuRu}_4\text{Sb}_{12}$ and $\text{EuOs}_4\text{Sb}_{12}$.

While the presence of a second peak at 6983 eV in the XANES spectra is sometimes observed in materials containing Eu^{2+} (i.e., EuF_2 (figure 7), EuS [22]), the peak is at nearly the same energy as the main peak in the Eu^{3+} spectra (i.e., EuF_3). Assuming this peak at 6983 eV to be attributable to Eu^{3+} , the XANES data for the three Eu-based filled skutterudites were fitted to a sum of two distinct Lorentzian peaks A(Eu^{2+}) and B(Eu^{3+}) (located at ~ 6974 and ~ 6982 eV respectively), including two ‘arctan’ functions for the edge step, as shown in figure 8 for $\text{EuOs}_4\text{Sb}_{12}$. In the fit, the distance and the amplitude ratio of the two Lorentzian peaks are constrained to be the same as those of the two arctan functions. The fraction of Eu^{3+} is then given by $I_B/(I_A + I_B)$. This analysis yields an upper limit of 9% Eu^{3+} in $\text{Eu}_{0.95}\text{Fe}_4\text{Sb}_{12}$ and $\text{EuRu}_4\text{Sb}_{12}$ and 10% Eu^{3+} in $\text{EuOs}_4\text{Sb}_{12}$. Eu L_{III} edge XANES data were recently reported by Grytsiv *et al* [23] for another Eu-based filled skutterudite system, $\text{Eu}_y\text{Fe}_{4-x}\text{Co}_x\text{Sb}_{12}$. From their results, a mixed valence state for the Eu ion was obtained by assuming that Eu^{3+} is solely responsible for the second peak at 6983 eV in the Eu L_{III} edge data. For these samples, the Eu valence decreases as the Eu concentration, y , increases, from $\nu = 2.6$ for 20% Eu to $\nu = 2.2$ for $\sim 85\%$ Eu [23]. Their linear extrapolation to 100% Eu yields $\nu \sim 2.07$ which agrees well with our value based on the above upper limit of $\nu = 2.09$ for $\text{Eu}_{0.95}\text{Fe}_4\text{Sb}_{12}$. No obvious T -dependence of the XANES spectra was found for all samples, which is consistent with previous measurements by Grytsiv *et al* [23].

4. Discussion

The thermodynamic and transport properties of $\text{EuRu}_4\text{Sb}_{12}$ and $\text{EuOs}_4\text{Sb}_{12}$ reveal ferromagnetic order below $T_C = 3$ and 8 K, respectively. The specific heat anomaly below T_C and the extended T -range of the Curie–Weiss behaviour $\chi(T)$ are consistent with a MFT description of the ferromagnetic state in these two compounds. The magnetic order in $\text{Eu}_{0.95}\text{Fe}_4\text{Sb}_{12}$ at $T_C = 87$ K does not appear to be associated with a simple ferromagnetic

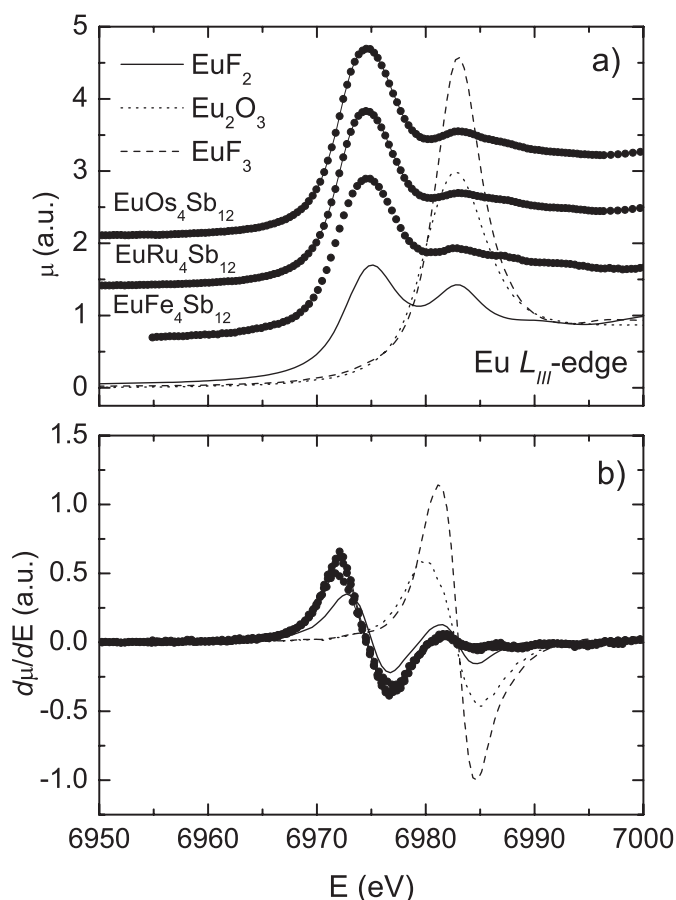


Figure 7. Panel (a): Eu L_{III} absorption edge spectra $\mu(E)$ for $\text{EuT}_4\text{Sb}_{12}$ ($T = \text{Fe, Ru, Os}$) and three Eu references EuF_2 (Eu^{2+}), EuF_3 (Eu^{3+}), and Eu_2O_3 (Eu^{3+}), at $T = 300$ K. The data for the Eu-based skutterudites have been shifted vertically for clarity. Panel (b): the derivative of the absorption spectra in panel (a) $d\mu/dE$ versus energy E .

structure due to the reduced saturation moment $\mu_{\text{sat}} = 5.1 \mu_{\text{B}}/\text{Eu}$, compared to the Eu^{2+} free ion value of $\mu_{\text{sat}} = 7.0 \mu_{\text{B}}/\text{Eu}$. Ferrimagnetic order involving the Eu and Fe moments, or a canted ferromagnetic structure, are consistent with the reduced value of μ_{sat} . In any case, a larger exchange coupling is found in $\text{Eu}_{0.95}\text{Fe}_4\text{Sb}_{12}$ relative to both $\text{EuRu}_4\text{Sb}_{12}$ and $\text{EuOs}_4\text{Sb}_{12}$; similar behaviour is found in $\text{EuFe}_4\text{P}_{12}$ which exhibits ferromagnetic order at $T_{\text{C}} = 99$ K [24] compared to $\text{EuRu}_4\text{P}_{12}$ with $T_{\text{C}} = 18$ K [24].

A number of investigations of the filled antimonide skutterudites suggest that Fe is paramagnetic in these materials. Magnetic measurements by Danebrock *et al* [9] on a number of alkaline-earth and lanthanide antimonide skutterudites, in which the R ion is nonmagnetic, i.e., $\text{RFe}_4\text{Sb}_{12}$ ($\text{R} = \text{Sr, Ca, Ba, La}$), yield an effective moment $\mu_{\text{eff}} = 3.0\text{--}4.0 \mu_{\text{B}}$. In the case of $\text{PrFe}_4\text{Sb}_{12}$ and $\text{NdFe}_4\text{Sb}_{12}$, the measured effective moment is larger than the free ion value of Pr^{3+} or Nd^{3+} , suggesting that Fe contributes to the magnetism in these compounds [25]. In addition, itinerant ferromagnetism has been reported in $\text{NaFe}_4\text{Sb}_{12}$ and $\text{KFe}_4\text{Sb}_{12}$ [19]. The effective moments in the intermediate valence compounds $\text{CeFe}_4\text{Sb}_{12}$ and $\text{YbFe}_4\text{Sb}_{12}$ are $\mu_{\text{eff}} = 3.5\text{--}3.8 \mu_{\text{B}}$ [26, 27] and $\mu_{\text{eff}} = 3.1\text{--}4.5 \mu_{\text{B}}$ [28, 29], respectively. For $\text{CeFe}_4\text{Sb}_{12}$, these

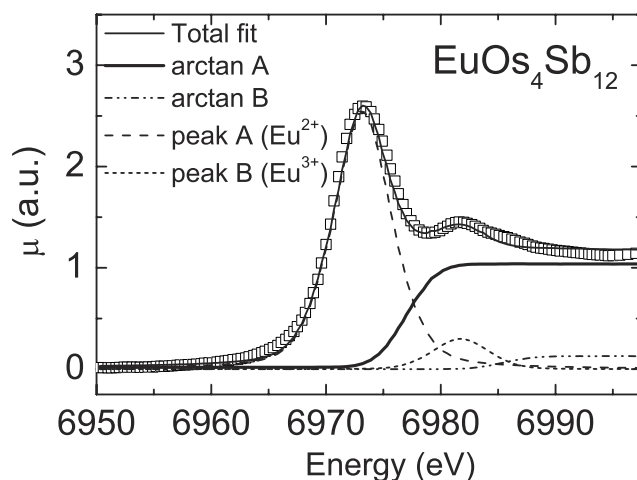


Figure 8. A fit of the XANES spectra of $\text{EuOs}_4\text{Sb}_{12}$ at 300 K. The open squares represent $\text{EuOs}_4\text{Sb}_{12}$ XANES data. The thin solid curve is the total fit result, while the dashed curve and dotted curve are the Eu^{2+} and Eu^{3+} peaks, respectively. The thick solid curve and dash-dotted curve are standard edge-step ‘arctan’ functions for the Eu^{2+} and Eu^{3+} , respectively.

values are larger than the effective moment expected from the intermediate valence state properties deduced from XANES measurements, i.e., $\mu_{\text{eff}} = 2.45 \mu_{\text{B}}$ for $\nu = 3.07$ [30] (assuming that $\chi(T)$ follows a linear relation with the valence ν), suggesting that Fe also has a magnetic moment in this material. In $\text{YbFe}_4\text{Sb}_{12}$, the filling fraction of the Yb site or the presence of tiny amounts of Yb_2O_3 [31] are probably responsible for the different values of μ_{eff} and the valence ($\nu = 2.68$ [29], $\nu = 2.33$ [30], or $\nu = 2.16$ [31]), but values of μ_{eff} are in general larger than expected from the mixed valence state determined from XANES measurements; for instance, a valence $\nu = 2.68$ implies an effective moment $\mu_{\text{eff}} = 3.75 \mu_{\text{B}}$ for $\text{Yb}_{1.0}\text{Fe}_4\text{Sb}_{12}$ compared to the experimental value $\mu_{\text{eff}} = 4.49 \mu_{\text{B}}/\text{fu}$ [29]. In addition, the magnetic properties of $\text{Co}_{1-x}\text{Fe}_x\text{Sb}_3$ ($x = 0-0.1$ [32], and 0.2 [27]) indicate that Fe is paramagnetic. Thus, it appears that Fe contributes to the magnetic properties of $\text{Eu}_{0.95}\text{Fe}_4\text{Sb}_{12}$, in the light of the number of other antimonide skutterudite compounds which suggest the presence of Fe moments. The magnetic susceptibility results presented here are consistent with an effective moment of the $(\text{Fe}_4\text{Sb}_{12})$ polyanion of $\mu_{\text{eff}}^{\text{poly}} = 3.8 \mu_{\text{B}}$ and a stable divalent Eu electronic configuration. The (nearly) divalent state of Eu in $\text{EuFe}_4\text{Sb}_{12}$ is supported by the weak temperature dependence of the XANES spectra and by ^{151}Eu Mössbauer measurements [10, 23]. Previous results on polycrystalline samples are also consistent with an $(\text{Fe}_4\text{Sb}_{12})$ polyanion contribution to $\chi(T)$, but could also be analysed assuming a mixed valence state of Eu [9, 10, 23].

In conclusion, we have studied the physical properties of single crystals of filled skutterudite compounds $\text{EuT}_4\text{Sb}_{12}$ ($T = \text{Fe}, \text{Ru}, \text{Os}$). Our results show that $\text{Eu}_{0.95}\text{Fe}_4\text{Sb}_{12}$ orders magnetically at $T_{\text{C}} = 87$ K, possibly in a ferrimagnetic or canted ferromagnetic structure, while $\text{EuRu}_4\text{Sb}_{12}$ and $\text{EuOs}_4\text{Sb}_{12}$ are ferromagnets with Curie temperatures of $T_{\text{C}} = 4$ and 9 K, respectively. The Eu XANES measurements on $\text{EuT}_4\text{Sb}_{12}$ ($T = \text{Fe}, \text{Ru}, \text{Os}$) suggest a nearly divalent Eu configuration in the temperature range $4-300$ K.

Acknowledgments

We would like to thank B C Sales for stimulating discussions. AŚ is grateful for the hospitality at UCSD and support from the Fulbright Foundation during his visit. Work at UCSD was

supported by the US Department of Energy under Grant No DE FG03-86ER-45230 and the NEDO International Joint Research Grant programme. Work at UCSC was supported by the National Science Foundation under Grant No DMR0071863. The XANES experiments were performed at SSRL, which is operated by the DOE, Division of Chemical Sciences, and by the NIH, Biomedical Resource Technology Program, Division of Research Resources.

References

- [1] Nolas G S, Morelli D T and Tritt T M 1999 *Annu. Rev. Mater. Sci.* **29** 89
- [2] Uher C 2001 *Recent Trends in Thermoelectric Research I* vol 69, ed T M Tritt (San Diego, CA: Academic) chapter 5, pp 139–253
- [3] Bauer E D, Ślebarski A, Freeman E J, Sirvent C and Maple M B 2001 *J. Phys.: Condens. Matter* **13** 4495 and references therein
- [4] Jeitschko W and Braun D 1977 *Acta Crystallogr. B* **33** 3401
- [5] Braun D J and Jeitschko W 1980 *J. Less-Common Met.* **72** 147
- [6] Shirota I, Shimaya Y, Kihou K, Sekine C and Yagi T 2003 *J. Solid State Chem.* **174** 32
- [7] Sekine C, Uchiumi T, Shirota I, Matsuhira K, Sakakibara T, Goto T and Yagi T 2000 *Phys. Rev. B* **62** 11581
- [8] See, for example, Falicov L M, Hanke W and Maple M B (ed) 1981 *Valence Fluctuations in Solids* (Santa Barbara, CA: Institute for Theoretical Physics)
- [9] Danebrock M E, Evers C B H and Jeitschko W 1996 *J. Phys. Chem. Solids* **57** 381
- [10] Bauer E, Berger S, Galatanu A, Galli M, Michor H, Hilscher G, Paul C, Ni B, Abd-Elmeguid M M, Tran V H, Grytsiv A and Rogl P 2001 *Phys. Rev. B* **63** 224414
- [11] Takeda N and Ishikawa M 2000 *J. Phys. Soc. Japan* **69** 868
- [12] Nonius Kappa CCD Program Package COLLECT, DENZO, SCALEPACK, SORTAV 1998 Nonius Delft, Netherlands
- [13] Sheldrick G M 1997 *SHELX-97, Program for Crystal Structure Refinement* University of Göttingen, Germany (*Windows version by McArdle* National University of Ireland, Galway, Ireland)
- [14] Li G G, Bridges F and Booth C H 1995 *Phys. Rev. B* **52** 6332
- [15] Bridges F, Booth C H and Li G G 1995 *Physica B* **208/209** 121
- [16] Sales B C, Chakoumakos B C, Mandrus D, Dilley N R and Maple M B 1998 *Thermoelectric Materials* vol 545, ed T M Tritt, M G Kanatzidis, G D Mahan and H B Lyon Jr (Warrendale, PA: Materials Research Society) p 13
- [17] Cao D, Bridges F, Chesler P, Bushart S, Bauer E D and Maple M B 2004 *Phys. Rev. B* submitted
- [18] Bauer E D, Ślebarski A, Dickey R P, Freeman E J, Sirvent C, Zapf V S and Maple M B 2001 *J. Phys.: Condens. Matter* **13** 5183
- [19] Leithe-Jasper A, Schnelle W, Rosner H, Senthilkumaran N, Rabis A, Baenitz M, Gippius A, Morozova E, Mydosh J A and Grin Y 2003 *Phys. Rev. Lett.* **91** 037208
- [20] Smart J S 1966 *Effective Field Theories of Magnetism* (Philadelphia, PA: Saunders)
- [21] Fishman R S and Liu S H 1989 *Phys. Rev. B* **40** 11028
- [22] Inoue T, Kubozono Y, Kashino S, Takabayashi Y, Fujitaka K, Hida M, Inoue M, Kanbara T, Emura S and Uruga T 2000 *Chem. Phys. Lett.* **316** 381
- [23] Grytsiv A, Rogl P, Berger S, Paul C, Bauer E, Godart C, Ni B, Abd-Elmeguid M M, Saccone A, Ferro R and Kaczorowski D 2002 *Phys. Rev. B* **66** 094411
- [24] Sekine C, Inoue M, Inaba T and Shirota I 2000 *Physica B* **281/282** 308
- [25] Bauer E, Berger S, Galatanu A, Paul C, Mea M D, Michor H, Hilscher G, Grytsiv A, Rogl P, Kaczorowski D, Keller L, Hermannsdörfer T and Fisher P 2002 *Physica B* **312/313** 840
- [26] Morelli D T and Meisner G P 1995 *J. Appl. Phys.* **77** 3777
- [27] Gajewski D A, Dilley N R, Bauer E D, Freeman E J, Chau R, Maple M B, Mandrus D, Sales B C and Lacerda A 1998 *J. Phys.: Condens. Matter* **10** 6973
- [28] Dilley N R, Freeman E J, Bauer E D and Maple M B 1998 *Phys. Rev. B* **58** 6287
- [29] Leithe-Jasper A, Kaczorowski D, Rogl P, Bogner J, Reissner M, Steiner W, Wiesinger G and Godart C 1999 *Solid State Commun.* **109** 395
- [30] Cao D, Bridges F, Baumbach R, Chesler P, Bauer E D, Ślebarski A and Maple M B 2004 unpublished
- [31] Bérardan D, Godart C, Alleno E, Berger S and Bauer E 2003 *J. Alloys Compounds* **351** 18
- [32] Yang J, Meisner G P, Morelli D T and Uher C 2000 *Phys. Rev. B* **63** 014410